Title
DECAY OF 209At TO LEVELS IN 209Po

Authors
Jardine, L.J.
Prussin, S.G.
Hollander, J.M.

Publication Date
1974-04-01

Submitted to Nuclear Physics

LBL-245
Preprint

DECAY OF ^{209}At TO LEVELS IN ^{209}Po

L. J. Jardine, S. G. Prussin and J. M. Hollander

April 1974

Prepared for the U. S. Atomic Energy Commission
under Contract W-7405-ENG-48

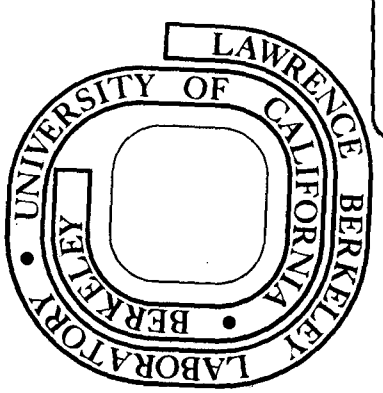

LBL-245

DISCLAIMER

DECAY OF ^{209}At TO LEVELS IN ^{209}Po†

L. J. Jardine and S. G. Prussin

Lawrence Berkeley Laboratory and
Department of Nuclear Engineering
University of California
Berkeley, California 94720

and

J. M. Hollander

Lawrence Berkeley Laboratory
University of California
Berkeley, California 94720

April 1974

Abstract

The electron-capture decay of ^{209}At has been investigated and present data define twenty-one levels in ^{209}Po. The multipolarity of thirty-six transitions have been deduced and combined with data from recent reaction studies to assign spins and parities to levels. Evidence is presented to identify seniority one and seniority three states below 2.3 MeV which arise from couplings of the one-neutron hole with two-proton configurations. A calculation using experimental data from neighboring isotopes in the lead region to approximate residual interactions was found to give remarkable agreement with the experimental level structure below 1.6 MeV. First-forbidden electron-capture transition rates to even parity levels at 2.3 and 2.9 MeV in ^{209}Po are discussed with reference to the $g_{9/2}$ and $i_{11/2}$ seniority one neutron states.

†Work performed under the auspices of the U. S. Atomic Energy Commission.

RADIOACTIVITY ^{209}At [from ^{209}Bi(α,4n)];
measured E_γ, I_γ, I_{ce}, γ-γ coinc; deduced
EC branching, log ft. ^{209}Po deduced levels,
J, π, cc, γ-multipolarity. Ge(Li), Si(Li) detectors, Ge(Li)-Ge(Li) coinc., mass spect.

1. Introduction

Theoretical calculations[1,2]) of the level structure of $^{210}_{84}Po$ and $^{210}_{82}Pb$ assuming two particles outside a $^{208}_{82}Pb$ core have been found to give remarkable agreement with the experimental[3,4]) level structures. Due to the proximity of $^{209}_{84}Po$ to these nuclei, one might hope to describe the low-lying level structure of ^{209}Po in terms of three-particle states arising from couplings of the odd-neutron with the two protons outside a lead core. The existence of such three particle states was first ascribed to ^{209}Po by Yamazaki and Matthias[5]) who investigated the $^{208}Pb(\alpha,3n\gamma)$ reaction. Later reports of the same reaction by Wikström[6]) and Bergström et al.[7]) have given further support to the existence of three particle states. A recent study[8]) of the $^{210}Po(d,t)^{209}Po$ and $^{210}Po(p,d)^{209}Po$ reactions has located low-lying levels which are predominantly of seniority one character. Although the electron-capture decay of ^{209}At is expected to populate intensely only a few levels which have large components of selected seniority one configurations, subsequent gamma decay should excite seniority three type states which are not readily observed in the stripping reactions. The decay and reaction studies thus complement each other and can provide a more complete understanding of the low-lying level structure of ^{209}Po.

In the present paper, we report on the investigation of the γ-ray transitions following the electron-capture decay of ^{209}At. The energies and intensities of approximately one hundred transitions between levels in ^{209}Po have been measured and multipolarities of thirty-six of these have been determined by measuring relative internal conversion coefficients. These data have been combined with results from gamma-gamma coincidence measurements to construct a decay scheme for ^{209}At. Together with the data obtained through reaction studies,

states arising from seniority three and seniority one configurations have been identified and the electron-capture decay to these levels are discussed in terms of the single-neutron states giving rise to first forbidden β-decay transitions. Finally, the level spectrum of ^{209}Po has been calculated using experimental matrix elements for proton-proton, proton-core, neutron-hole-proton, and neutron-hole-core interactions obtained from analysis of the level structure of nuclei adjacent to ^{208}Pb. The calculated spectrum below 1.7 MeV in excitation-energy compares remarkably well with the experimental level spectrum.

During the course of our study a number of reports of similar investigations have appeared in the literature[9,10,11,12,13]. While our data compare favorably with the results from these studies, especially regarding the more intense γ-ray transitions, a number of significant differences are noted and these are discussed in the main text.

2. Experimental

2.1. SOURCES

Sources used in this study were obtained by the reaction $^{209}Bi(\alpha,4n)^{209}At$ at bombarding energies of 47-51 MeV with bismuth metal targets of thicknesses 30-59 mg/cm^2. Chemical purification of the astatine was achieved by volatilization as previously described[12,14]. Due to the broad excitation functions for the (α,xn) reactions, sources prepared in this way contained varying amounts of ^{208}At, ^{210}At, and ^{211}At. While the contribution from ^{208}At could be minimized by reducing the beam energy below the $(\alpha,5n)$ threshold, these sources contained unacceptibly high fractions of ^{210}At activity, and, as a result, it was necessary to deduce the γ-ray transitions following ^{209}At decay by analysis of fairly complex spectra. The γ-ray transitions of ^{208}At and ^{210}At were identified by comparison of energies and intensities with the data reported by Treytl, Hyde, and Yamazaki[15] and Jardine, Prussin, and Hollander[3]. To confirm assignments made to the ^{209}At spectrum and to search for additional weak transitions, a low-intensity source of ^{209}At was prepared by mass separation in the Berkeley Isotope Separator. No γ-ray transitions were detected from this source other than those from the decay of the ^{209}At and its decay products.

Two types of sources were used for conversion electron measurements. When astatine was obtained by the volatilization procedure, solutions containing the ^{209}At were evaporated onto aluminum-coated mylar which was then coated with a thin (3-10 μg/cm^2) layer of aluminum to prevent migration of the astatine in the vacuum chamber of the electron detector. For the mass separated ^{209}At, a narrow strip from the aluminum collection plate was used directly as a source.

2.2. GAMMA-RAY SPECTRA

Gamma-ray singles spectra in the energy range of 100-2700 keV were obtained with a 35-cm^3 (system resolution 2.6 keV (FWHM) at 1332 keV) coaxial Ge(Li) detector. For measurements in the energy range of 16-500 keV a 10-cm^3 planar Ge(Li) detector (system resolution 1.5 keV (FWHM) at 122 keV) and a 0.784 cm^2 × 5 mm Si(Li) detector (system resolution 0.8 keV (FWHM) at 60 keV) were employed. All measurements were taken with conventional high-rate pulse electronics[16,17]) coupled to a 4096-channel analog-to-digital converter of the successive approximation type[18]). A PDP-7 computer system[19,20,21]) was used for on-line analysis. Typical γ-ray spectra are shown in figs. 1, 2, and 3. The spectra were analyzed with the computer code SAMPO[22]) and energy calibration was obtained with the data compiled by Jardine[23]). Uncertainties due to the relative efficiency calibrations of the various detectors were estimated to be ±5% in the energy range of 100-600 keV and ±4% in the energy range of 500-2800 keV[24]). The energies and intensities of γ-ray transitions definitely assigned to the decay of ^{209}At are given in Table 1 and a list of possible additional weak transitions assigned tentatively through analysis of the spectrum obtained with the mass separated source is given separately in Table 2. Absolute transition intensities were obtained from the intensity balance of the decay scheme and with corrections for internal conversion of the low energy transitions with known multipolarities obtained with the theoretical conversion coefficients of Hager and Seltzer[25]). For several of the low-energy transitions of uncertain multipole character, it was necessary to assume values consistent with placement of the transitions in the decay scheme. (The transitions at energies of 90.8, 113.2, and 151.5 keV were all assumed to be pure E2 transitions. The 90.8 keV γ-ray

was not resolved from the K_β X-rays of polonium with the detectors employed in this study. The reported γ-ray intensity has been calculated from the measured intensities of the L-conversion electrons which established this transition to be of E2 multipolarity.)

The data reported here are generally in good agreement with those reported by Alpsten, Appelqvist, and Astner[9] (AAA), Charvet et al.[10], and Afansev et al.[11]. A number of discrepancies are, however, worthy of note. The γ-ray transitions at energies of 1096.0, 1333.4, 2105, and 2204 keV assigned to the decay of ^{209}At by AAA[9]) were not observed in our measurements. We can set sufficiently low intensity limits for these to conclude that they probably do not follow the ^{209}At decay. This argument is also used to rule against the tentative assignments by AAA[9]) of transitions at 807.4, 895.0, 2111, and 2448 keV to the decay of ^{209}At. We have found that the transition reported by AAA[9]) at 1147.6±0.2 keV (with a relative photon intensity of 2.4±0.1) can be resolved into a doublet of lines at energies of 1147.4±0.3 and 1148.8±0.3 keV with relative photon intensities of 1.5±0.1 and 0.86±0.10, respectively. Finally, the discrepancies between the intensities reported for the 104.2 keV transition is not considered serious and the lower value for the intensity of the 985.2 keV γ-ray reported in this work may reflect a correction for a contribution from the decay of ^{205}Bi.

2.3. INTERNAL CONVERSION ELECTRON SPECTRA

Spectra of conversion electrons were obtained with a 0.785 cm^2 × 5 mm lithium-drifted silicon detector (operated at liquid nitrogen temperature) coupled to the same data acquisition system and pulse electronics used in the γ-ray singles measurements (see section 2.2). This system gave a resolution of 1.2 keV

(FWHM) for 100 keV electrons and 2.2 keV (FWHM) for the K-conversion electron line of the 1063 keV transition in the decay of ^{207}Bi. Electron spectra were analyzed for energies and intensities with the computer code SAMPO[22]) with the K-electron lines of the stronger transitions used for internal energy calibration. The relative electron efficiency function of this detector was determined to ±4% over the energy range of 100-1500 keV and ±7% over the range of 1200-1700 keV using the methods described elsewhere[26]).

Some typical conversion electron spectra obtained with the mass separated source are shown in figs. 4 and 5. Both these and spectra obtained from unseparated sources were used for extraction of electron intensities. The electron intensities obtained from

these measurements were combined with measured γ-ray intensities to determine conversion coefficients relative to the K-conversion coefficient for the 545.0 keV ($5/2^- \rightarrow 1/2^-$) ground-state transition. This transition was assumed to be of pure E2 character[5]) and absolute values for all conversion coefficients were then obtained through use of the theoretical value of $\alpha_K(E2)$ for this transition. These are given in Table 3 along with the multipolarity assignments deduced by comparison with the theoretical values[25]). The experimental K-conversion coefficients are also shown in fig. 6 with the theoretical curves constructed from the values of ref. [25]). We comment further on several of our results in the following paragraphs.

2.3.1. 90.8 keV transition. The measured ratio $(\alpha_{L_1} + \alpha_{L_2})/\alpha_{L_3}$ for this transition establishes the multipolarity as E2 in agreement with previous results[9,10]). The total transition intensity and the intensity of the 90.8 keV γ-ray were then obtained by comparison of the total L-conversion electron intensity with the K-electron intensity of the 545.0 keV transition.

2.3.2. 195.0 keV transition. The M1-E2 mixing ratio M1 + ≈20%E2 for the 195.0 keV transition was determined from the ratio of our measured K and M+... conversion coefficients. The experimental ratio was 19.2±4.7 and the theoretical ratio for M1 + 20%E2 is α_K/α_M = 19.4. Our value of α_K is in agreement with AAA[9]).

2.3.3. 551.0 and 552.4 keV transitions. The K-conversion electrons of these two transitions were not resolved in our spectra. Using our relative γ-ray intensities and assuming the 551.0 keV transition to be pure E2 as required by our decay scheme (section 3), the α_K of the 552.4 keV transition was calculated from the sum electron intensity to be 0.086±0.10 which is consistent with M1 multipolarity.

2.3.4. 1147.4 and 1148.8 keV transitions. As discussed in subsection 2.2, these were detected as an unresolved doublet for which we were not able to resolve the K-electrons. Both our γ-ray and conversion electron sum intensities agree with AAA[9]). If we assume that the 1148.8 keV transition is of E1 multipolarity as suggested by the level scheme of section 3, we calculate an α_K = 0.005±0.001 for the 1147.4 keV transition which implies E2 multipolarity. These results remain tentative but consistent with our level scheme.

2.4. GAMMA-GAMMA COINCIDENCE MEASUREMENTS

Three parameter γ-γ coincidence measurements of a mixed source were taken with two coaxial Ge(Li) detectors of about 35 cm^3 each (active volume).

The axes of the two detectors were positioned at 90° with respect to the sources and were separated by a graded shield (lead-cadmium-copper) to minimize scattering between the detectors. A fast-coincidence electronic arrangement was used similar to that described by Jaklevic et al.[27]) with the width of the prompt time distribution determined by the 545.0-781.9 keV γ-ray cascade of about 40 nsec (FWHM). Three parameter data (E_1, E_2, Δt) were stored serially on magnetic tape and later sorted on the LBL CDC-6600 computer system. The sorting routine employed permitted subtraction of random events and events associated with the neighboring Compton distributions from each energy gate with sorts performed at a resolving time of about 80 nsec. Several typical coincidence spectra are shown in figs. 7 and 8 with the complete set given in ref. [12]).

3. The Decay Scheme

Coincidence measurements and the sum-difference relationships among γ-ray energies have been used to construct the level scheme shown in fig. 9. Spin and parity assignments are based upon previously reported data[5,9]), our conversion electron measurements and the results of the ^{210}Po(d,t)^{209}Po and ^{210}Po(p,d)^{209}Po reaction studies[8]). The electron-capture branching ratios to the various ^{209}Po levels were calculated from the total transition intensity depopulating each level using our relative γ-ray intensity data corrected for internal conversion and assuming no β-decay to the ground state. Where no β-branching was indicated, limits were determined from intensity errors and these are shown as dashed lines in fig. 9. Log ft values were obtained by using the method discussed by Konopinski and Rose[28]). The Q-value[29]) used for the electron-capture decay was 3483±9 keV and the half-life[30]) was taken as 5.42±0.06 hours. The mode of the ^{209}At decay was taken[31]) as 95.9% EC and 4.1±0.5% α decay.

As discussed in section 4 below, the low-lying level spectrum can be characterized by seniority one and seniority three states arising from the couplings of a single neutron hole to two proton configurations, and we discuss the level spectrum below with reference this description. As an aid to the discussion we show in fig. 10 the experimental (neutron-hole) states of ^{207}Pb which may be compared directly to levels in ^{209}Po assigned as seniority one states. We also include in that figure a portion of the level spectrum observed[8]) in the ^{210}Po(d,t)^{209}Po reaction which is characterized by states believed to have dominant seniority one structures.

3.1. LEVELS OF SENIORITY ONE AT 0.0, 545.0, 854.4, 1761.1, AND 2312.2 keV

The ground state and levels at 545.0, 854.4, and 1761.1 keV were strongly populated[8]) in the reaction ^{210}Po(d,t)^{209}Po, with cross sections comparable to

those observed for excitation of single neutron-hole states in the $^{208}Pb(p,d)^{207}Pb$ reaction. The transitions to these states in ^{209}Po were assigned definite ℓ-transfers of 1, 3, 1, and 6, respectively. The spin of the ground state has been measured[32]) as 1/2 and by analogy with the levels in ^{207}Pb, the angular momentum transfers fix the spins of the other three levels as 5/2(545.0), 3/2(854.4), and 13/2(1761.1). These four levels are identified with the seniority one configurations $(\pi(h_{9/2})^2_0\ \nu(p_{1/2})^{-1})_{1/2^-}$, $(\pi(h_{9/2})^2_0\ \nu(f_{5/2})^{-1})_{5/2^-}$, $(\pi(h_{9/2})^2_0\ \nu(p_{3/2})^{-1})_{3/2^-}$, and $(\pi(h_{9/2})^2_0\ \nu(i_{13/2})^{-1})_{13/2^+}$.

The spin and parity of the level at 2312.2 keV is fixed at $9/2^+$ by observation of decay to the levels at 545.0 and 1761.1 keV by M2 and E2 transitions, respectively. This level receives about 75% of the intensity in the electron-capture decay of ^{209}At by an unhindered, first forbidden transition (log ft = 6.1). As previously pointed out[9,33]), electron capture of nuclides in the immediate vicinity of ^{208}Pb probe core excited states and it is likely that the level at 2312.2 keV arises from the dominant configuration $(\pi(h_{9/2})^2_0\ \nu(g_{9/2})^1)_{9/2^+}$. This interpretation is consistent with the fact that this level was not observed in the $^{210}Po(d,t)$ reaction studies[8]), as the $g_{9/2}$ orbital is expected to be almost empty in the ^{210}Po (target) ground state.

The transitions shown in fig. 9 arising from the decay of these excited seniority one levels are in agreement with those placed in the decay schemes of AAA[9]) and Charvet[10]) with two notable exceptions. The transition at 342.8 keV has not been placed between the $9/2^+$ state at 2312.2 keV and the $13/2^-$ state at 1417.8 keV. If this placement were correct, then the transition energy should be the sum of those at 104.2 and 239.2 keV. A precise determination of these γ-ray energies with ^{133}Ba and ^{182}Ta as internal standards[23]) gave the following sum relations:

$$(104.187\pm0.003)_\gamma + (239.190\pm0.018)_\gamma = (343.377\pm0.020)_{sum} \neq (342.87\pm0.008)_\gamma$$

which is also in agreement with the values given by AAA[9])

$$(104.1\pm0.1)_\gamma + (239.1\pm0.1)_\gamma = (343.2\pm0.2)_{sum} \neq (342.8\pm0.1)_\gamma \ .$$

Further, our experimental α_K implies a multipolarity of E1 + ≈10%M2 or E2 + ≈30%M1 and the latter would be inconsistent with this placement in the decay scheme. The transition may be an unresolved doublet and at this time we have no energy sum or definitive coincidence information upon which a placement in the decay scheme can be based.

We also note that the 596.4 keV transition can be placed in two different locations in the level scheme on the basis of energy sums. We favor the tentative placement (based on very weak γ-γ coincidence results) between the $9/2^+$ state at 2312.2 keV and $9/2^-$ state at 1715.8 keV which would suggest an E1 multipolarity. However, the experimental α_K is consistent with either E1 + ≈15%M2 or E2 + ≈30%M1. Thus, either the transition has two components with some intensity belonging to each placement or there must be an M2 component in strong competition with the E1.

3.2. LEVELS OF SENIORITY THREE BELOW 2 MeV

The theoretical calculations presented in section 4 suggest that additional states below 2 MeV in ^{209}Po can be assigned dominant configurations of the type $\pi(h_{9/2})^2_{J\neq0}\ \nu(\ell_j)$ and all additional observed levels in this energy range are shown to be of odd parity. Detailed arguments for spin and parity assignments to these levels are given below.

3.2.1. Levels at 1175.4, 1326.9, 1409.1, 1417.8, 1522.0, 1715.8, and 1991.2 keV. The parity of the level at 1175.4 keV is established as odd and its spin limited to 3/2 or 5/2 by the 630.3 keV (M1) and 1175.4 keV (E2) transitions to the first-excited and ground states, respectively. The (M2) character of the transition at 1136.5 keV from the $9/2^+$ level at 2312.2 keV establishes a definite $5/2^-$ assignment to the 1175.4 keV level. This level was weakly populated[8]) through an $\ell = 3$ transfer in the ^{210}Po(d,t) reaction which is believed to result from configuration mixing with the $5/2^-$ seniority one level at 545.0 keV.

The angular distribution measurements of Yamazaki and Matthias[5]) establish the spin and parity of the level at 1326.9 keV as $9/2^-$. The measured E2 multipolarity of the 781.9 keV transition from this level to $5/2^-$ first excited state is consistent with this assignment.

The level at 1409.1 keV was established by definition of the 903.05-233.7-1175.4 γ-ray cascade through coincidence measurements. The 903.05 keV (E1) transition from the $9/2^+$ level at 2312.2 keV and the 233.7 keV (M1) transition to the $5/2^-$ level at 1175.4 keV fix the spin and parity as $7/2^-$. Similarly, the spin and parity of the level at 1522.0 keV is defined as $11/2^-$ by the 239.2 keV (E1) transition from $13/2^+$ level at 1761.1 keV and by the 195.0 keV (M1 + E2) transition to the $9/2^-$ level at 1326.9 keV.

The level at 1417.8 keV was strongly excited in the ^{208}Pb(α,3nγ) reaction studies by Bergström et al.[7]), indicating a high value for the spin of this level. An odd parity and a spin assignment in the range 9/2-13/2 are assigned to this level through the M1 character of the 104.2 keV transition and the E2 character of the 90.8 keV transition. We note further that the measured ratio

$(\alpha_{L_1} + \alpha_{L_2})/\alpha_{L_3}$ for the latter transition is consistent with an assignement of pure E2, the assumption of which would lead to a definite assignment of $13/2^-$ for the spin and parity of the 1417.8 keV level. While this remains somewhat tentative, it is consistent with all experimental data.

The levels at 1715.8 keV and 1991.2 keV were also established from coincidence data. A definite assignment of $9/2^-$ for the spin and parity of the 1715.8 keV level results from the measured multipolarities of the 1170.75 keV (E2) and 388.9 keV (M1) transitions to the levels at 545.0 and 1326.9 keV, and through population by the 1148.8 keV (E1) transition from the $11/2^+$ level at 2864.6 keV (see section 3.3). The level at 1991.2 keV is assigned the spin and parity of $7/2^-$ through the measured multipolarities of the 815.6 keV (M1) and 321.1 keV (E1) transitions. A level at 1996 keV was excited[8]) in the ^{210}Po(d,t) reaction via an $\ell = 3$ transfer. Our spin and parity assignment is consistent with this result if the 1991.2 keV level is assumed to be that observed in the reaction experiments.

3.2.2. Level at 1213.8 keV. A level at 1214 keV was weakly populated (presumably thru an admixture of the seniority one $3/2^-$ state at 854.4 keV) in the ^{210}Po(d,t) reaction[8]) with an $\ell = 1$ transfer, implying a spin and parity assignment of $(1/2,3/2)^-$ for this level. We have observed a weak γ-ray at an energy of 1213.8 keV in the decay of ^{209}At and tenatively assign this as the ground state transition in the decay of the same level. The theoretical calculations given in section 4 support this level and the assignment of $3/2^-$ for the spin and parity.

3.3. EVEN PARITY LEVELS AT 2864.6, 2902.5, 2908.5, AND 2978.5 keV

The even parity nature of these levels is readily established through the measured multipolarities of γ-ray transitions arising in their decay and log ft values for electron-capture decay to these levels are consistent with first-forbidden transitions. A spin of 11/2 is assigned to the level at 2864.6 keV through decay to the 2312.2 keV ($9/2^+$) and 1761.1 keV ($13/2^+$) levels by the transitions of 552.4 keV (M1) and 1103.5 keV (M1 + E2), respectively. The 1141.4 keV M1 transition to the $13/2^+$ state at 1761.1 keV limits the spin of the 2902.5 keV level to 11/2, 13/2, 15/2. However, the relatively low log ft of 7.1 for electron-capture decay to this level and the weak 2357.7 keV transition to the 545.0 keV $5/2^-$ level argue strongly for the lower spin assignment of 11/2.

The probable multipolarity assignments of (E1) to the 1581.6 keV transition populating the $9/2^-$ level at 1326.9 keV and (E2) to the 1147.4 keV transition to the $13/2^+$ state at 1761.1 keV limit the spin and parity of the 2908.5 keV level to $9/2^+$, $11/2^+$. The log ft value of 6.6 for electron-capture decay to this level is consistent with these assignments.

The 1262.6 keV (E1) transition to the $9/2^-$ level at 1715.8 keV limits the spin of the level at 2978.4 keV to 7/2, 9/2, 11/2. The tentative assignment of (M1 + E2) for the multipolarity of the 1217.2 keV transition to the $13/2^+$ level at 1761.1 keV and the low log ft value of 6.4 argue for an assignment of 11/2 for the spin of this level.

3.4. LEVELS AT 2654.4, 2836.0, 3072.8, AND 3251.9 keV

The levels at 2654.4 and 3072.8 keV have been placed in the decay scheme on the basis of sum-difference relations between γ-ray energies, while the level at 2836.0 keV resulted from a weak coincidence between 1074.8 and 239.2 keV

γ-rays. While the lack of multipolarity assignments to γ-ray transitions arising from these levels precludes definite assignments of spins and parities, we note that the presence of a ground state transition in the decay of the 2654.4 keV level along with the measured log ft of 8.6 for electron-capture decay limit likely assignments to $5/2^{\pm}$ or $7/2^{+}$.

4. Calculation of the Level Spectrum of ^{209}Po Using Experimental Two-Nucleon Matrix Elements

The calculation of the energies of high spin states in ^{210}Po using experimental level energies and ground state nuclear masses to estimate matrix elements for proton-proton interactions has reproduced a partial level spectrum in excellent agreement with experimental data[34]). Similar calculations applied to high spin states of other nuclei in the vicinity of ^{208}Pb have also reproduced experimental spectra with sufficient quality[35,36]), that it is of some interest to consider how well this calculational technique reproduces the complete level spectrum at low excitation energies. The basic assumptions underlying this approach are that the Hamiltonian can be written as a sum of two-body interactions which are identical to those in neighboring nuclei, and that configuration mixing may be neglected.

We have used this technique to calculate the level spectrum of ^{209}Po with the assumption that the low-lying level spectrum is describable in terms of two proton-one neutron hole states. Matrix elements for proton-proton and neutron hole-proton interactions were taken from experimental data[3,37]) on the energy levels of ^{210}Po and ^{208}Bi, respectively, while those for proton-core and neutron-hole-core interactions were estimated from the level spectra of ^{209}Bi and ^{207}Pb, respectively. With these four interactions, the mass $M^I(^{209}\text{Po})$ of a state of total spin I, formed from the coupling of the three particle momenta $((j_{\pi_1}\ j_{\pi_2})_J\ j_\nu)I$ may be written as

$$M^{I}(^{209}\mathrm{Po}) = M^{(j_{\pi_1}\, j_{\pi_2})J}(^{210}\mathrm{Po}) + M^{j_\nu}(^{207}\mathrm{Pb}) - M^{0^+}(^{208}\mathrm{Pb})$$

$$+ \sum_{J'} (2J+1)(2J'+1)\left|W(j_{\pi_1}\, j_{\pi_2}\, I\, j_\nu\, ;\, J\, J')\right|^2 \Delta M^{J'}_{j_{\pi_1}\, j_\nu}$$

$$+ \sum_{J''} (2J+1)(2J''+1)\left|W(j_{\pi_2}\, j_{\pi_1}\, I\, j_\nu\, ;\, J\, J'')\right|^2 \Delta M^{J''}_{j_{\pi_2}\, j_\nu} \qquad (1)$$

where

$$\Delta M^{J'} = M^{(j_{\pi_1}\, j_{\pi_2})J'}(^{208}\mathrm{Bi}) + M^{0^+}(^{208}\mathrm{Pb}) - {}^{j_{\pi_1}}M(^{209}\mathrm{Bi}) - {}^{j_\nu}M(^{207}\mathrm{Pb}) \qquad (2)$$

and

$$\vec{I} = \vec{J} + \vec{j}_\nu \quad , \quad \vec{J} = \vec{j}_{\pi_1} + \vec{j}_{\pi_2} \quad , \quad \text{and } \vec{J}' = \vec{j}_{\pi_1} + \vec{j}_\nu \quad . \qquad (3)$$

The mass (or energy) to be used in the above equations is the ground state mass plus the energy of the excited state with the appropriate spin. (The W(j j' I j"; J J') are Racah coefficients.) The energies of levels calculated with eq. (1) below 2 MeV in excitation are compared with the experimental spectrum in fig. 11. We have also included in that figure the level spectrum obtained from the shell model calculation of Baldridge et al.[38]) which permits some qualitative evaluation of the relative importance of configuration mixing in this energy range.

It is evident from the data shown in fig. 11, that the simple calculation using experimental matrix elements compares quite favorably with the more sophisticated shell model calculation and both reproduce the experimental level

scheme quite well. With the exceptions of the lowest lying levels of spin 13/2 and 7/2, the calculation reproduces the same spin sequence of levels that are experimentally observed in the region below 1.7 MeV of excitation energy.

The neglect of configuration mixing in the calculations presented here are evident, especially with regard to the energy of the seniority one level, $(\pi(h_{9/2})^2_{0^+}\ \nu(p_{3/2})^{-1})_{3/2^-}$, at 854.4 keV. The calculation of Baldridge et al.[38], which reproduces the experimental energy more accurately, indicates extensive configuration mixing between this state and the seniority three state $(\pi(h_{9/2})^2_{2^+}\ \nu(p_{1/2})^{-1})_{3/2^-}$ observed experimentally[8] at 1214 keV. The leading terms of the wave function for the 854.4 keV level as obtained from the shell model calculation[38] were

$$0.863\,|(\pi_{9/2})^2_{0^+}\ \nu(p_{3/2})^{-1})\,3/2^-> + 0.453\,|(\pi(h_{9/2})^2_{2^+}\ \nu(p_{1/2})^{-1})\,3/2^-> + \ldots$$

It is of interest to note here that while both $3/2^-$ levels were excited in the ^{210}Po(d,t) reaction[8], the level at 1214 keV was only weakly populated, presumably through the (small) amplitude of the seniority one configuration contained in the state. A similar situation is apparent relative to configuration mixing between the two lowest $5/2^-$ levels, although the disagreement is not as pronounced. Again both states were excited in the ^{210}Po(d,t) reaction but relatively weakly in the case of the level at 1175 keV.

As a result of the comparison of the predictions of the two calculations with the experimental reaction[5,6,8] and radioactive decay data, the seniority one states corresponding to the configurations $\pi(h_{9/2})^2_{0^+}\ \nu(\ell_j)$ where $\nu(\ell_j) \equiv p^{-1}_{1/2}$, $f^{-1}_{5/2}$, $p^{-1}_{3/2}$, $i^{-1}_{13/2}$, and $g_{9/2}$ are now identified as are all of the

states of the seniority three configurations $(\pi(h_{9/2})^2_{J\neq 0} \nu(p_{1/2}^{-1}))$ with the single exception of the $15/2^-$ member of this set. The lack of definite spin assignments and the expected high level density above 1.7 MeV of excitation energy presently preclude identification of seniority three states arising from the dominant configurations $(\pi(h_{9/2})^2_{J\neq 0} \nu(f_{5/2})^{-1})$ and $(\pi(h_{9/2})^2_{J\neq 0} \nu(p_{3/2})^{-1})$. Configuration mixing is certainly of more importance in this energy range, and as a result the seniority one configuration $(\pi(h_{9/2})^2_{0^+} \nu(f_{7/2})^{-1})_{7/2^-}$ is probably fragmented over several states near 2 MeV. The ^{210}Po(d,t) reaction data[8]) indicated a relatively strong $\ell = 3$ transfer to a level at 1996 keV and it is likely that this level may correspond to our level at 1991.2 keV and contain some of the strength of this $7/2^-$ configuration.

5. Electron-Capture Decay Rates

Electron-capture decay of ^{209}At should favor transitions to seniority one states in ^{209}Po where the transitions are relatively unhindered. The ground state of $^{209}_{85}At^{124}$ is presumed to have the dominant configuration $(\pi(h_{9/2})^3_{9/2^-}\ \nu(f_{5/2})^6_{0^+})_{9/2^-}$ and consequently strong decay to levels containing large components of the seniority one configurations $(\pi(h_{9/2})^2_0\ \nu(g_{9/2})^1)_{9/2^+}$ and $(\pi(h_{9/2})^2_0\ \nu(i_{11/2})^1)_{11/2^+}$ are expected to proceed via unhindered first-forbidden transitions. Decay to other seniority one configurations should be highly hindered because of the large change in orbital angular momentum in these cases.

The $9/2^+$ level at 2312.2 keV has been assigned as having the dominant configuration $(\pi(h_{9/2})^2_0\ \nu(g_{9/2})_{9/2^+})_{9/2^+}$ and it is populated by electron-capture decay with a log ft = 6.1. This value is comparable in magnitude to that observed[3]) for the same transitions ($\pi h_{9/2} \rightarrow \nu g_{9/2}$) seen in the electron-capture decay of ^{210}At to ^{210}Po.

A number of levels at about 3 MeV in ^{209}Po are populated by electron-capture transitions of relatively low log ft values, and it is probable that these proceed via components of the seniority one configuration $(\pi(h_{9/2})^2_0\ \nu(i_{11/2})_{11/2})_{11/2^+}$. From the energy spacing of the $g_{9/2}$ and $i_{11/2}$ neutron orbitals derived from the spacings[37,39]) of the $9/2^+$ ground state and the $11/2^+$ first excited state in ^{209}Pb (778 keV) and in ^{211}Po (687 keV), this configuration is expected to lie near 3 MeV in ^{209}Po. Configuration mixing with other even parity states in the vicinity can be expected to produce substantial fragmentation because of the level density.

Acknowledgments

The authors wish to acknowledge the generous assistance given by Drs. C. M. Lederer and G. L. Struble. We would also like to thank Dr. M. C. Michel for performing the mass separations. One of us (LJJ) wishes to acknowledge financial support from the Atomic Energy Commission in the form of a Nuclear Science and Engineering Fellowship during a period of this study.

References

1) C. W. Ma and W. W. True, Phys. Rev. C8 (1973) 2313

2) M. G. Redlich, Phys. Rev. 138 (1965) B544

3) L. J. Jardine, S. G. Prussin, and J. M. Hollander, Nucl. Phys. A190 (1972) 261

4) E. R. Flynn, G. J. Igo, R. A. Broglia, S. Landowne, V. Paar, and B. Nilsson, Nucl. Phys. A195 (1972) 97

5) T. Yamazaki and E. Matthias, Phys. Rev. 175 (1968) 1476

6) K. Wikström, Research Institute for Physics, Stockholm, Annual Report (1971), p. 87

7) I. Bergström, B. Fant, C. J. Herrlander, K. Wikström, and P. Thieberger, Research Institute for Physics, Stockholm, Annual Report (1969), p. 49

8) T. S. Bhatia, T. R. Canada, C. Ellegaard, J. Miller, E. Romberg, and P. D. Barnes, Bull. Am. Phys. Soc. 16 (1971) 1147; private communications, November 1971, January 1972, July 1972, and February 1974

9) M. Alpsten, A. Appelqvist, and G. Astner, Physica Scripta 4 (1971) 137

10) A. Charvet, R. Chery, D. H. Phuoc, R. Duffiat, A. Einsallem, and G. Marguier, Comp. Rend. 290B (1972) 274

11) V. P. Afanasev et al., Izv. Akad. Nauk SSSR, Ser. Fiz. 37 (1973) 25; Izv. Akad. Nauk SSSR, Ser. Fiz. 37 (1973) 31

12) L. J. Jardine, Ph.D. Thesis, Lawrence Berkeley Laboratory Report LBL-245 (1971)

13) L. J. Jardine, S. G. Prussin, and J. M. Hollander, Lawrence Berkeley Laboratory Report LBL-1666 (1972)

14) E. H. Appleman, National Academy of Sciences National Research Council Report NASA-NS-3012 (1960)

15) W. J. Treytl, E. K. Hyde, and T. Yamazaki, Nucl. Phys. A117 (1968) 481

16) F. S. Goulding, University of California, Lawrence Radiation Laboratory Report UCRL-17559 (1967)

17) F. S. Goulding, D. A. Landis, and R. H. Pehl, University of California, Lawrence Radiation Laboratory Report UCRL-17560 (1967)

18) L. B. Robinson, F. Gin, and F. S. Goulding, University of California, Lawrence Radiation Laboratory Report UCRL-17419 (1967)

19) L. B. Robinson and J. D. Meng, University of California, Lawrence Radiation Laboratory Report UCRL-17220 (1967)

20) J. O. Radeloff, L. B. Robinson, and J. D. Meng, University of California, Lawrence Radiation Laboratory Report UCRL-18883 (1969)

21) F. M. Bernthal, Ph.D. Thesis, University of California, Lawrence Radiation Laboratory Report UCRL-18651 (1969)

22) J. R. Routti and S. G. Prussin, Nucl. Instr. Methods 72 (1969) 125

23) L. J. Jardine, University of California, Lawrence Radiation Laboratory Report UCRL-20476 (1971)

24) L. J. Jardine, Nucl. Instr. Methods 96 (1971) 259

25) R. S. Hager and E. C. Seltzer, Nucl. Data A4 (1968) 1

26) L. J. Jardine and C. M. Lederer, Lawrence Berkeley Laboratory Report LBL-208 (1974), submitted to Nucl. Instr. Methods, March 1974

27) J. M. Jaklevic, F. M. Bernthal, J. O. Radeloff, and D. A. Landis, Nucl. Instr. Methods 69 (1969) 109

28) E. J. Konopinski and M. E. Rose, in Alpha-, Beta-, and Gamma-Ray Spectroscopy, Vol. 2, ed. by K. Siegbahn, North-Holland, Amsterdam (1965), p. 1357

29) A. H. Wapstra and N. B. Gove, Nucl. Data A9 (1971) 267

30) S. Geutkh, B. S. Dzhelepov, Y. V. Norseev, and V. A. Khalkin, Program and Theses, Proc. 18th Ann. Conf. Nucl. Spectroscopy and Structure of At. Nuclei, Riga (1968) 96

31) N. A. Golovkov, S. Guetkh, B. S. Dzhelepov, Y. V. Norseev, V. A. Khalkin, and V. G. Chumin, Izv. Acad. Nauk SSSR, Ser. Fiz. 33 (1969) 1622

32) K. L. Vander Sluis and P. M. Griffin, J. Opt. Soc. Am. 45 (1955) 1087

33) S. G. Prussin and J. M. Hollander, Nucl. Phys. A110 (1968) 176

34) J. Blomqvist, B. Fant, K. Wikström, and I. Bergström, Phys. Scripta 3 (1971) 9

35) I. Bergström, C. J. Herrlander, P. Thieberger, and J. Blomqvist, Phys. Rev. 181 (1969) 1642

36) J. Blomqvist, Research Institute for Physics, Stockholm, Annual Report (1972), p. 164

37) M. R. Schmorak, R. L. Auble, M. B. Lewis, and M. J. Martin, Nucl. Data B5 (1971) 207

38) W. Baldridge, N. Freed, and J. Gibbons, Phys. Letters 36B (1971) 179

39) L. J. Jardine, unpublished results (1972)

40) L. A. Sliv and I. M. Band, Coefficients of Internal Conversion of Gamma Radiation, Academy of Sciences of the USSR, Moscow-Leningrad, Part I, K-Shell (1956); Part II, L-Shell (1958)

Table 1 . Gamma-rays observed in the decay of ^{209}At.

γ-ray Energy (keV)	Relative[a] γ-ray intensity	Relative[b] transition intensity
90.8 (2)	(2.0 (2))[c]	(23.9 (25))[c]
104.2 (2)	2.20 (25)	(15.8 (E2) 25.1 (M1))
113.2 (3)	0.18 (4)	(0.97)[d]
151.5 (3)	0.06 (2)	(0.14)[d]
191.1 (3)[e]	0.41 (7)	–
195.0 (1)	24.2 (12)	60.1 (32)[f]
233.7 (1)	1.10 (9)	2.33 (18)
239.2 (1)	13.5 (5)	14.2 (7)
321.1 (2)	0.69 (3)	0.70 (4)
342.8 (2)[e]	0.57 (3)	0.67 (5)
388.9 (2)	0.54 (3)	0.68 (5)
415.8 (6)[g]	0.06 (2)	–
433.8 (3)[g]	0.08 (2)	–
447.7 (2)	0.29 (2)	0.34 (3)

γ-ray Energy (keV)	Relative[a] γ-ray intensity	γ-ray Energy	Relative[a] γ-ray intensity
545.0 (1)	100	1272.9 (2)[e]	0.22 (2)
551.0 (3)	5.4 (2)	1311.7 (3)	0.056 (6)
552.4 (4)	1.6 (2)	1342.9 (3)[e,h]	0.071 (6)
554.6 (4)	0.70 (11)	1357.0 (2)	0.18 (1)

(continued)

Table 1 (continued)

γ-ray Energy (keV)	Relative[a] γ-ray intensity	γ-ray Energy (keV)	Relative[a] γ-ray intensity
596.4 (2)	0.72 (4)	1409.0 (6)[g]	0.019 (8)
630.3 (2)	0.75 (3)	1411.1 (4)[e,i]	0.058 (8)
666.2 (1)	2.04 (7)	1427.0 (3)[g]	0.031 (6)
719.6 (3)[e]	0.08 (1)	1446.15 (10)	0.58 (2)
750.9 (2)[e]	0.07 (1)	1456.4 (2)	0.12 (1)
781.9 (1)	91.7 (26)	1478.9 (3)	0.044 (4)
790.2 (1)	69.9 (20)	1484.7 (3)[g]	0.10 (1)
799.1 (2)[e]	0.11 (2)	1490.8 (2)	0.29 (2)
809.8 (3)[e,i]	0.036 (8)	1533.1 (2)[e]	0.17 (1)
815.6 (3)	0.25 (3)	1537.7 (1)	0.54 (4)
817.7 (3)[e,g]	0.18 (4)	1575.6 (2)	0.92 (4)
826.8 (3)[e,i]	0.05 (1)	1581.6 (1)	1.95 (7)
854.4 (2)	0.64 (4)	1622.4 (2)[e]	0.18 (1)
864.0 (1)	2.24 (10)	1651.5 (5)	0.043 (4)
903.05 (10)	4.00 (12)	1687.3 (2)[e]	0.41 (2)
910.7 (5)[e,i]	0.077 (11)[j]	1730.0 (4)[g]	0.013 (2)
922.0 (3)[e,i]	0.077 (10)	1745.8 (3)	0.090 (5)
939.5 (3)[g]	0.05 (1)	1767.0 (1)	0.54 (3)
985.2 (2)	0.8 (1)[j]	1786.5 (2)[e]	0.13 (1)
999.6 (2)[e]	0.17 (1)	1803.8 (2)[e]	0.058 (4)
1008.4 (4)[e,i]	0.038 (9)	1810.0 (2)[e]	0.043 (4)

(continued)

Table 1 (continued)

γ-ray Energy (keV)	Relative[a] γ-ray intensity	γ-ray Energy (keV)	Relative[a] γ-ray intensity
1037.8 (4)[e,i]	0.030 (6)	1861.4 (5)[e,k]	0.008 (2)
1074.8 (2)	0.21 (2)	1947.7 (4)[e]	0.015 (2)
1092.8 (4)[e]	0.049 (7)	2109.5 (3)	0.045 (4)
1103.46 (10)	5.93 (20)	2245.8 (6)[e]	0.007 (1)
1136.5 (3)	0.075 (10)	2292.3 (5)[e,i]	0.014 (4)[ℓ]
1141.4 (3)	0.34 (2)	2319.6 (4)	0.008 (2)
1147.4 (3)	1.50 (10)	2342.9 (4)[e]	0.021 (5)
1148.8 (3)	0.86 (10)	2357.7 (6)	0.006 (2)
1170.75 (10)	3.3 (1)	2363.7 (4)	0.015 (2)
1175.4 (2)	2.1 (1)	2368.3 (4)[e]	0.012 (2)
1183.0 (3)[e,g]	0.16 (2)	2433.44 (20)	0.015 (2)
1192.9 (3)	0.16 (4)	2528.1 (6)	0.003 (1)
1213.8 (2)	0.47 (4)	2555.4 (4)[e]	0.002 (1)
1217.2 (2)	1.20 (8)	2588.9 (4)[e]	0.021 (3)
1243.9 (2)[e]	0.17 (2)	2645.6 (3)[e]	0.013 (4)
1262.6 (1)	2.07 (8)	2654.4 (4)	0.003 (1)

(continued)

Table 1 (continued)

[a] Absolute γ-ray intensities (derived from the level scheme) may be obtained by renormalizing the relative intensities: The 545.0 keV transition has an absolute photon intensity of 94.4±2.0 per 100 decays of ^{209}At.

[b] The theoretical conversion coefficients of Hager and Seltzer[25]) were used to derive these transition intensities.

[c] These intensities were calculated from the relative conversion electron intensities where the 90.8 keV transition was assumed to be pure E2 (subsection 2.3.1).

[d] The multipolarity of this transition was assumed E2 for this table.

[e] These transitions are unplaced in the present level scheme.

[f] The multipolarity of this transition was assumed M1 + 20%E2 based on our measured values of α_K, α_L, and α_M (subsection 2.3.2).

[g] Assignment to ^{209}At decay is based on the observation of the transition in a low intensity ^{209}At mass separated source with no ^{210}At present.

[h] Assignment to ^{209}At decay is uncertain.

[i] This transition was observed as a very weak transition in mixed ^{210}At and ^{209}At sources and also in the low intensity ^{209}At mass separated source; however the assignment to ^{209}At decay is still uncertain.

[j] The intensity was corrected for a ^{205}Bi component.

[k] Assignment to ^{209}At decay is uncertain (^{205}Bi?).

[ℓ] The intensity was corrected for a ^{226}Ra component from room-background.

Table 2. Possible additional weak transitions observed from a low intensity mass separated ^{209}At source. The assignment of these transitions to ^{209}At decay is tentative and these are not placed in the current level scheme.

γ-ray Energy keV	Relative[a] γ-ray intensity
515.1 (3)	0.05 (2)
523.0 (3)	0.04 (2)
1084.0 (4)	0.037 (5)
1112.9 (6)	0.022 (6)
1202.3 (4)	0.022 (6)
1210.2 (4)	0.047 (10)
1295.8 (4)	0.026 (6)
1299.0 (5)	0.022 (6)
1361.7 (6)	0.009 (4)
1419.4 (4)	0.042 (9)
1421.5 (5)	0.023 (8)
1529.4 (5)	0.016 (5)
1706.1 (7)	0.006 (3)
2102.0 (4)	0.008 (3)

[a]The γ-ray intensity normalization is the same as Table 1.

Table 3. Experimental and theoretical internal conversion coefficients: ^{209}At.

Transition energy keV	Experimental[a] conversion coefficient (10^{-3})	Theoretical[b] conversion coefficient E1(10^{-3})	E2(10^{-3})	M1(10^{-3})	M2(10^{-3})	Assigned multipolarity
90.8	$(\alpha_{L_1} + \alpha_{L_2})/\alpha_{L_3}$ = 1340 (100)	3130	1300	142000	4100	E2
195.0	α_K = 1170 (120)	70.9	178	1420	5910	
	α_L = 220 (20)	13	256	250	1800	M1 + ≈20%E2
	α_M = 61 (7)	3.06	67.4	58.9	456	
233.7	α_K = 760 (50)	46	119	855	3230	
	α_L = 136 (10)	8.22	120	151	910	M1
	(α_M = 28 (10))[c]	1.93	31.5	35.5	229	
239.2	α_K = 37 (4)	43.5	113	801	2990	
	α_L = 5.0 (10)	7.75	109	141	834	E1
321.1	(α_K = 26 (15))[c]	22	58	357	1150	E1
342.8	α_K = 110 (10)	19	30.1	299	935	E2 + ≈30%M1 or E1 + ≈10%M2
388.9	α_K = 190 (20)	14.4	28.1	213	631	M1
447.7	α_K = 130 (20)	10.7	21	146	410	M1
523.0	(α_K = 320 (80))[d]	7.73	20.4	96.6	257	(M2)[d]

(continued)

Table 3 . (continued)

Transition energy keV	Experimental[a] conversion coefficient (10^{-3})	Theoretical[b] conversion coefficient E1(10^{-3})	E2(10^{-3})	M1(10^{-3})	M2(10^{-3})	Assigned multipolarity
545.0	$\alpha_K \equiv 18.7$[a]		18.7			(assumed E2)[a]
551.0	18.3[e]	6.96	18.3	84.3	228	E2[e]
552.4	86 (10)[e]	6.92	18.2	83.6	221	M1[e]
596.4	α_K = 31 (5)	5.94	15.6	68.4	175	E1 + ≈15%M2 or E2 + ≈30%M1
630.3	α_L = 13.5 (40)	0.859	3.83	10.2	31.1	M1
666.2	α_K = 13 (2) α_L = 3.0 (8)	4.79 0.768	12.6 3.29	51.2 8.79	128 26.3	E2
719.6	(α_K = 130 (40))[d]	4.14	10.9	41.9	103	(M2)[d]
781.9	α_K = 9.1 (7) α_L = 1.9 (2)	3.54 0.560	9.26 2.10	33.8 5.62	81.4 15.7	E2
790.1	α_K = 3.3 (3) α_L = 0.50 (7)	3.47 0.549	9.08 2.04	32.9 5.46	79 15.2	E1

(continued)

Table 3 . (continued)

Transition energy keV	Experimental[a] conversion coefficient (10^{-3})	Theoretical[b] conversion coefficient E1(10^{-3})	E2(10^{-3})	M1(10^{-3})	M2(10^{-3})	Assigned multipolarity
815.6	(α_K = 29 (8))[c]	3.27	8.55	30.3	72.3	(M1)[c]
817.7	(α_K = 16 (8))[c]	3.26	8.51	30.1	71.8	(M1 + E2)[c]
854.4	α_K = 26 (5)	3.00	7.84	26.9	63.7	M1
903.1	α_K = 3.3 (4)	2.71	7.07	23.3	54.8	E1
1103.5	α_K = 9.0 (9) α_L = 1.6 (4)	1.90 0.294	4.89 0.954	13.9 2.36	32.0 6.03	M1 + E2
1136.5	(α_K = 37 (12))[d]	1.8	4.63	12.9	29.3	(M2)
1141.4	α_K = 19 (6)	1.79	4.59	12.8	28.9	M1
1147.4	5±1[f]	1.77	4.55	12.6	28.9	E2[f]
1148.8	1.77[f]	1.77	4.54	12.6	28.8	E1[f]
1170.7	α_K = 4.6 (6) α_L = 0.94 (32)	1.71 0.264	4.39 0.838	12.0 2.03	27.4 5.12	E2

(continued)

Table 3 . (continued)

Transition energy keV	Experimental[a] conversion coefficient (10^{-3})	Theoretical[b] conversion coefficient E1(10^{-3})	E2(10^{-3})	M1(10^{-3})	M2(10^{-3})	Assigned multipolarity
1175.4	α_K = 4.9 (8)	1.70	4.35	11.9	27.1	E2
1213.8	(α_K = 6.8 (20))[c]	1.61	4.11	10.9	25.0	(M1 + E2)[c]
1217.2	(α_K = 7.1 (20))[c]	1.60	4.09	10.9	24.8	(M1 + E2)[c]
1262.6	α_K = 1.8 (4)	1.50	3.82	9.89	22.5	E1
1446.1	(α_K = 4.4 (10))[d]	1.19	2.99	7.0	15.9	(M1 + E2)[d]
1581.6	(α_K = 0.87 (40))[d]	1.03	2.55	5.57	12.7	(E1)[d]
1767.0	α_K = 9.6 (20)	0.854[g]	2.01[g]	3.96[g]	9.3[g]	M2

(continued)

Table 3 . (continued)

[a]These conversion coefficients were measured relative to that for the 545.0 keV ($5/2^- \rightarrow 1/2^-$) transition which was assumed to be ' pure E2.

[b]Theoretical values were obtained by computer interpolation from the tables of Hager and Seltzer[25]).

[c]This value was extracted from a complex (doublet) peak and is tentative due to poor resolution.

[d]This conversion coefficient is uncertain.

[e]These values were obtained as stated in subsection 2.3.3.

[f]These values were obtained as stated in subsection 2.3.4.

[g]This theoretical conversion coefficient was obtained by extrapolation from the tables of Sliv and Band[40]).

Figure Captions

Fig. 1. Gamma-ray spectrum of ^{209}At in the energy range of 100-1570 keV. Transitions not belonging to ^{209}At decay are marked with symbols: Δ ^{208}At, □ ^{210}At.

Fig. 2. Gamma-ray spectrum of ^{209}At in the energy range of 620-2660 keV. Transitions not belonging to the ^{209}At decay are marked with symbols: □ ^{210}At.

Fig. 3. Gamma-ray spectrum of ^{209}At (mass separated) in the energy range of 100-2700 keV.

Fig. 4. Conversion-electron spectrum (top) and X-ray spectrum (bottom) of ^{209}At (mass separated) in the energy range of 16-240 keV taken with a Si(Li) spectrometer. (The bottom spectrum was taken with teflon absorber covering the electron source.)

Fig. 5. Conversion-electron spectrum of ^{209}At (mass separated) in the energy range of 80-1800 keV.

Fig. 6. Comparison of the experimental K-conversion coefficients with the theoretical values of Hager and Seltzer[25]). The values for M2 transitions were extrapolated (dotted line) to 1770 keV.

Fig. 7. Gamma-ray spectra in coincidence with the 666.2, 903.1, and 1446.2 keV transitions. These helped to establish levels at 2978.4, 1409.1, 1175.4, and 1991.2 keV.

Fig. 8. Gamma-ray spectra in coincidence with the 1575.6, 1581.6, and 1767.0 keV transitions. These helped establish the levels at 2602.5 and 2608.5 keV as well as the placement of the 1767.0 keV M2 transition.

Fig. 9. Experimental decay scheme of ^{209}At. Relative photon intensities with their uncertainties in italics are shown above the transitions. Dashed lines with limits represent only the maximum possible β-branchings based on feedings from experimental γ-ray intensity errors.

Fig. 10. Comparison of the experimental[6,7]) level scheme of ^{209}Po (b) with the levels[37]) of ^{207}Pb (a) and the states populated[8]) (c) in the ^{210}Po(p,d)^{209}Po and ^{210}Po(d,t)^{209}Po reactions.

Fig. 11. Comparison of the experimental level scheme of ^{209}Po (b) with a shell model calculation (a)[38]) and with the calculation discussed in section 4, (c).

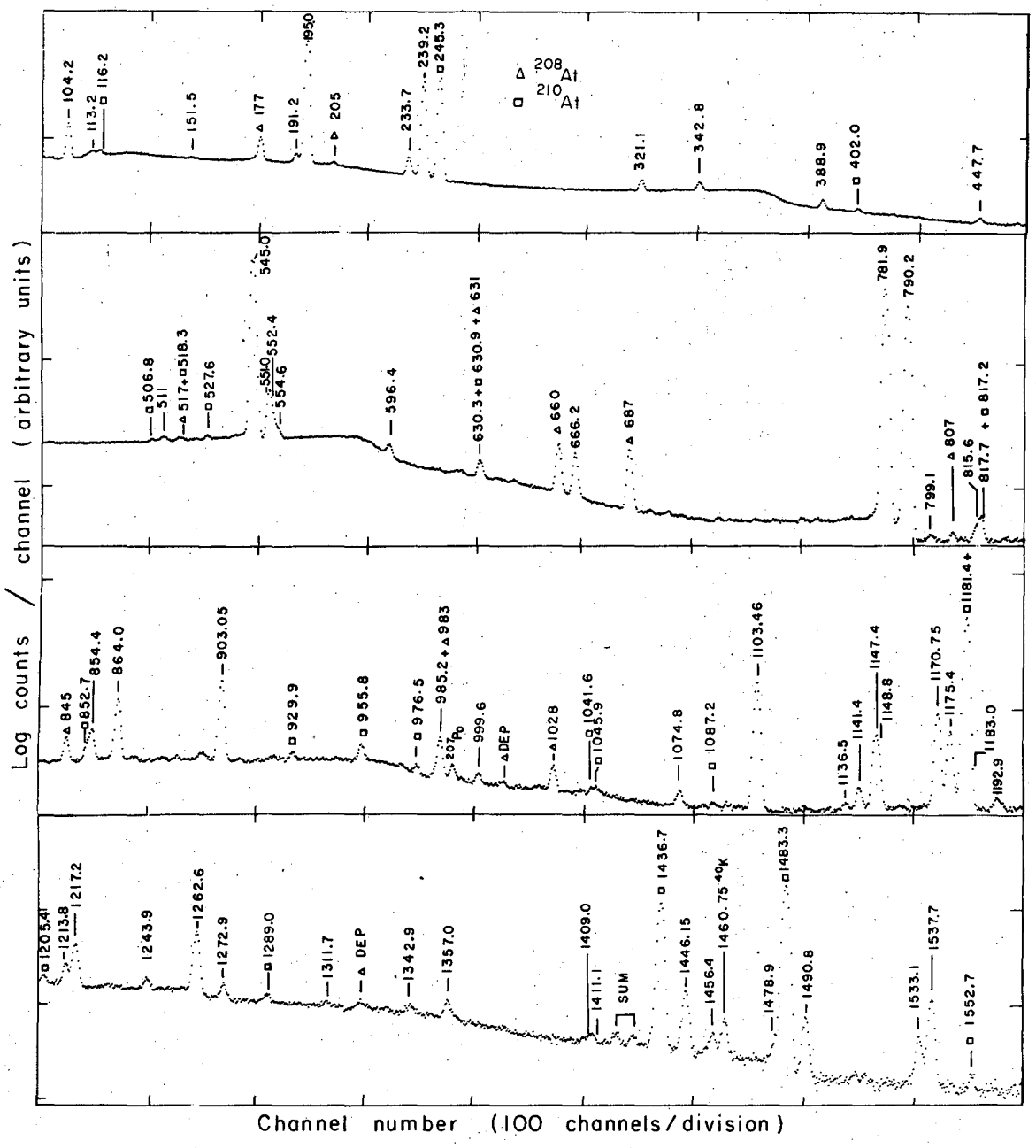
Log counts / channel (arbitrary units)
Channel number (100 channels/division)
Δ 208At
□ 210At
104.2
113.2
□ 116.2
151.5
Δ 177
191.2
205
233.7
239.2
□ 245.3
321.1
342.8
388.9
□ 402.0
447.7
□ 506.8
511
Δ 517+□ 518.3
□ 527.6
545.0
550
552.4
554.6
596.4
630.3+□ 630.9+Δ 631
Δ 660
666.2
Δ 687
781.9
790.2
799.1
Δ 807
815.6
817.7 + □ 817.2
Δ 845
852.7
854.4
864.0
903.05
□ 929.9
□ 955.8
□ 976.5
985.2+Δ 983
207Pb
999.6
Δ DEP
Δ 1028
□ 1041.6
□ 1045.9
1074.8
□ 1087.2
1103.46
1136.5
1141.4
1147.4
1148.8
1170.75
1175.4
□ 1181.4+
1183.0
1192.9
□ 1205.4
1213.8
1217.2
1243.9
1262.6
1272.9
□ 1289.0
1311.7
Δ DEP
1342.9
1357.0
1409.0
1411.1
SUM
□ 1436.7
1446.15
1456.4
1460.75 40K
□ 1483.3
1478.9
1490.8
1533.1
1537.7
□ 1552.7
XBL 7111-4723

Fig. 1

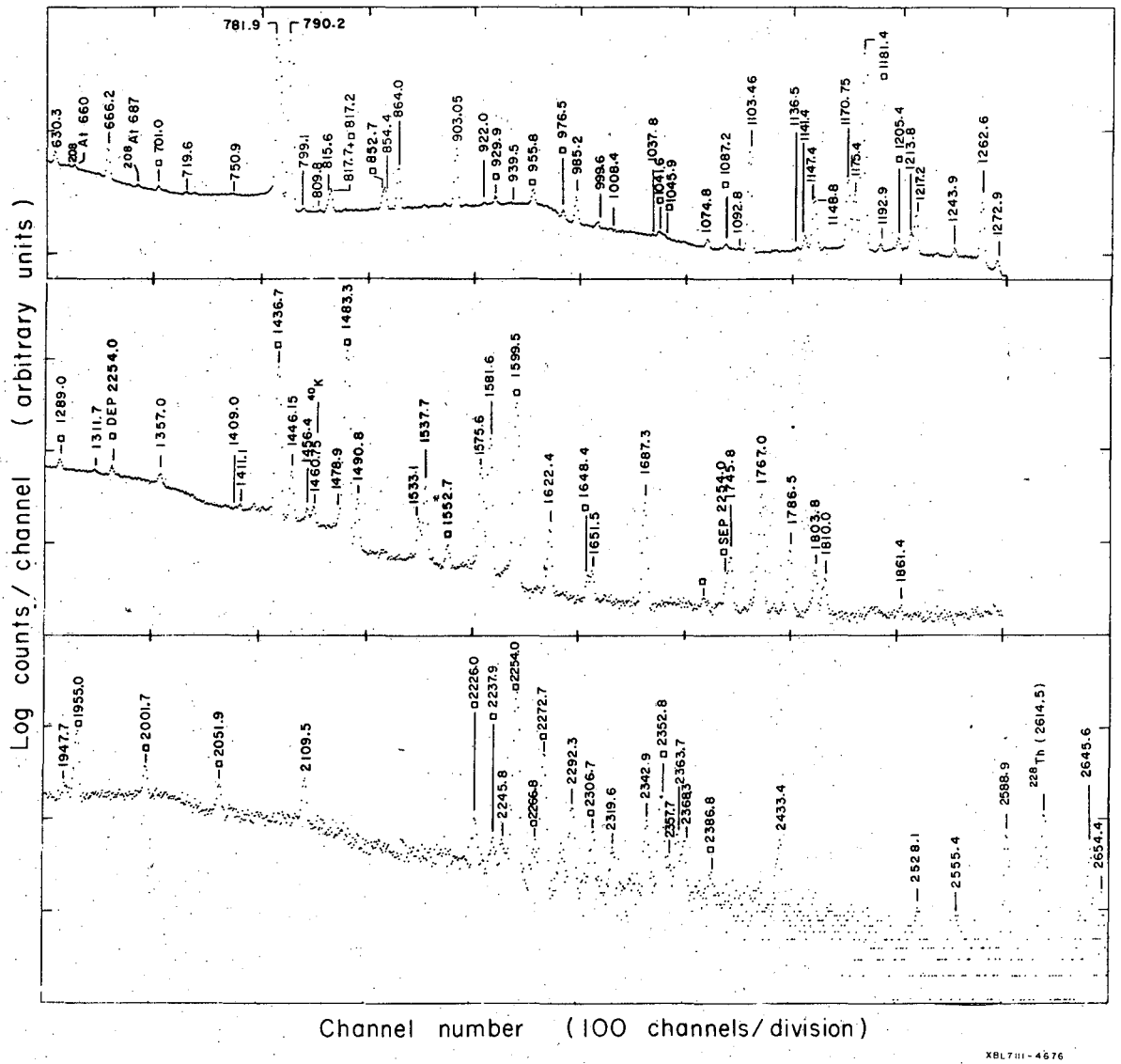
Log counts / channel (arbitrary units)
Channel number (100 channels/division)
781.9
790.2
630.3
Al 660
666.2
Al 687
701.0
719.6
750.9
799.1
809.8
815.6
817.7+817.2
852.7
854.4
864.0
903.05
922.0
929.9
939.5
955.8
976.5
985.2
999.6
1008.4
1037.8
1041.6
1045.9
1074.8
1087.2
1092.8
1103.46
1136.5
1141.4
1147.4
1148.8
1170.75
1175.4
1181.4
1192.9
1205.4
1213.8
1217.2
1243.9
1262.6
1272.9
1289.0
1311.7
DEP 2254.0
1357.0
1409.0
1411.1
1436.7
1446.15
1456.4
1460.75
40K
1478.9
1483.3
1490.8
1533.1
1537.7
1552.7
1575.6
1581.6
1599.5
1622.4
1648.4
1651.5
1687.3
SEP 2254.0
1745.8
1767.0
1786.5
1803.8
1810.0
1861.4
1947.7
1955.0
2001.7
2051.9
2109.5
2226.0
2237.9
2245.8
2254.0
2266.8
2272.7
2292.3
2306.7
2319.6
2342.9
2352.8
2357.7
2363.7
2368.3
2386.8
2433.4
2528.1
2555.4
2588.9
228Th (2614.5)
2645.6
2654.4
XBL7111-4676

Fig. 2

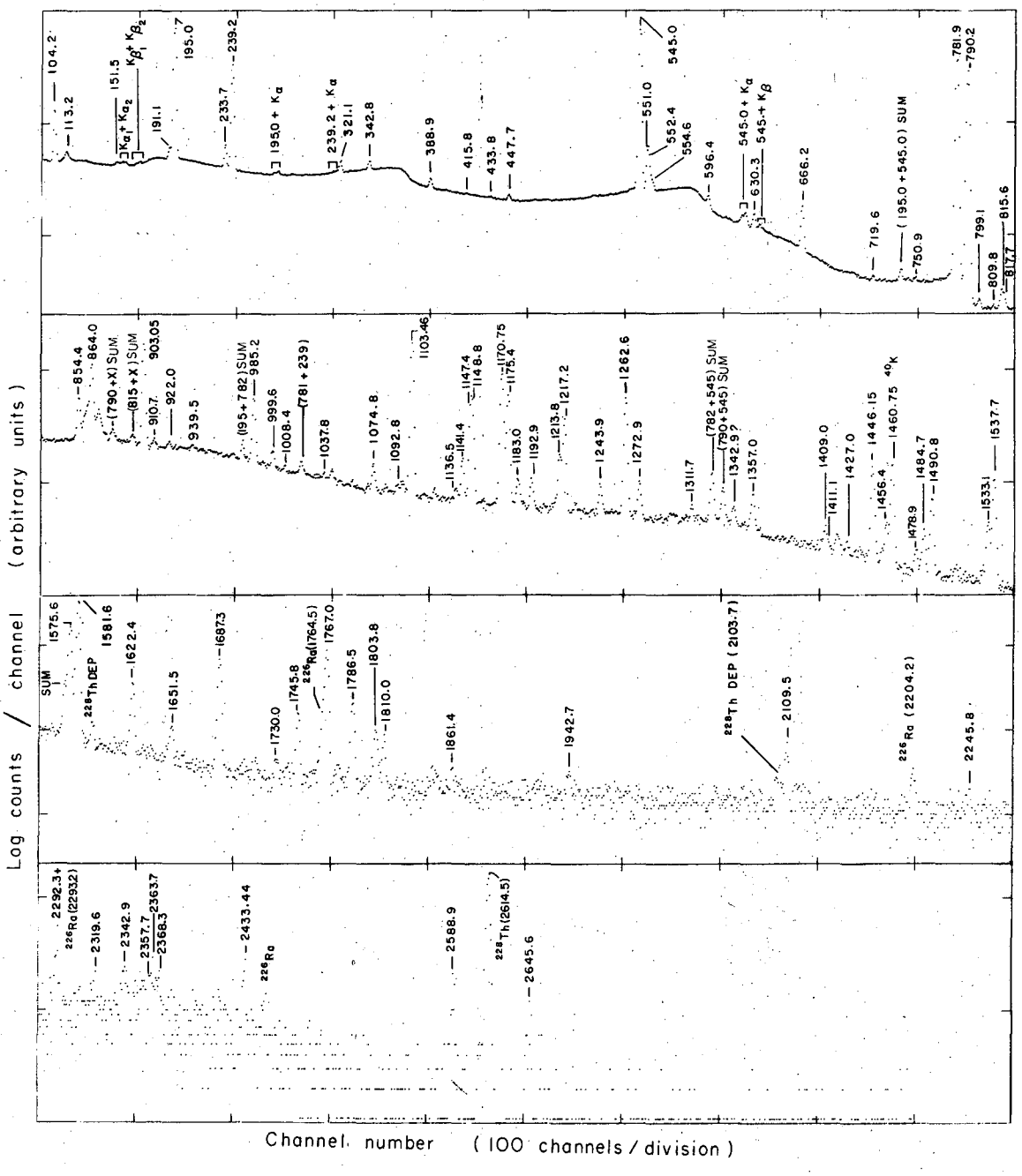
Log counts / channel (arbitrary units)
Channel number (100 channels / division)
XBL711-4726

Fig. 3

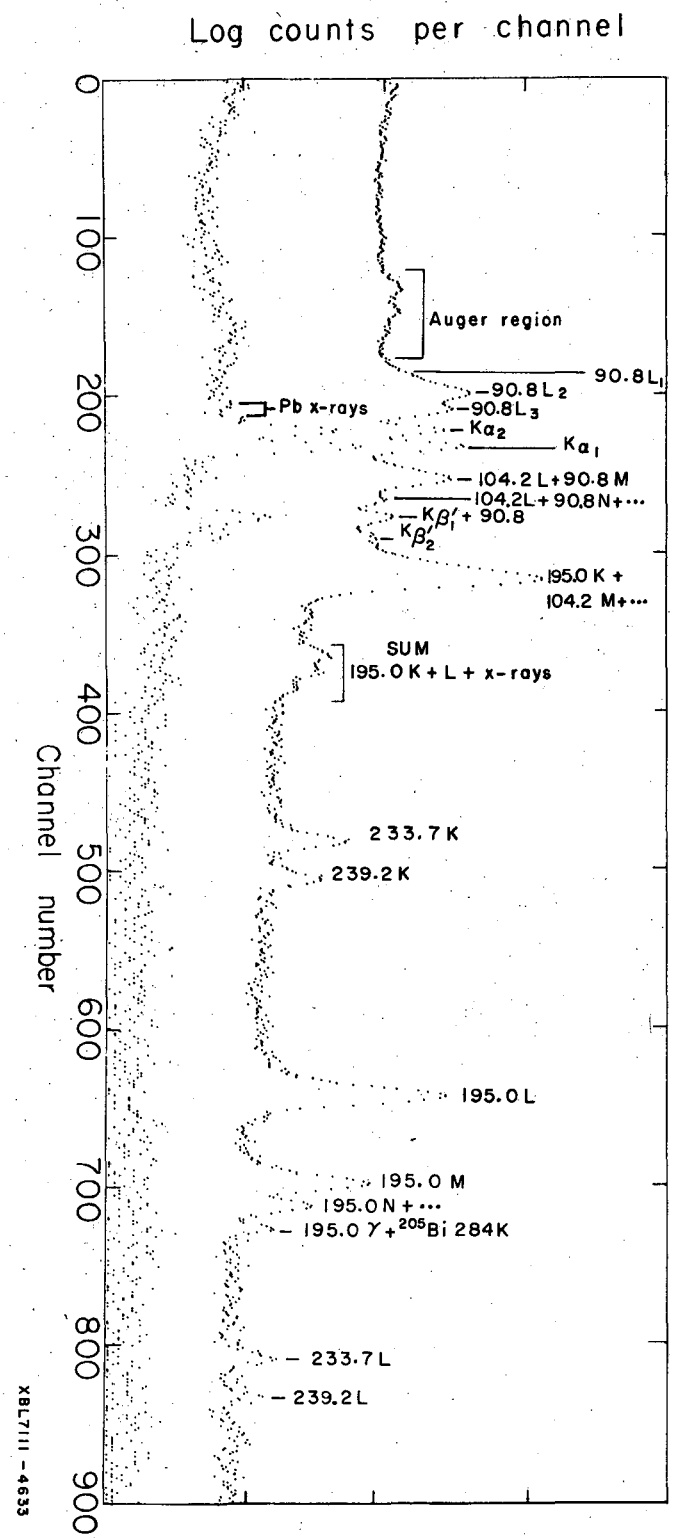
Log counts per channel
Channel number
0
100
200
300
400
500
600
700
800
900
Auger region
90.8 L1
90.8 L2
90.8 L3
Pb x-rays
Kα2
Kα1
104.2 L+90.8 M
104.2L+90.8N+···
Kβ1'+ 90.8
Kβ2'
195.0 K +
104.2 M+···
SUM
195.0 K + L + x-rays
233.7 K
239.2 K
195.0 L
195.0 M
195.0 N+···
195.0 γ+205Bi 284K
233.7 L
239.2 L
XBL7111-4633

Fig. 4

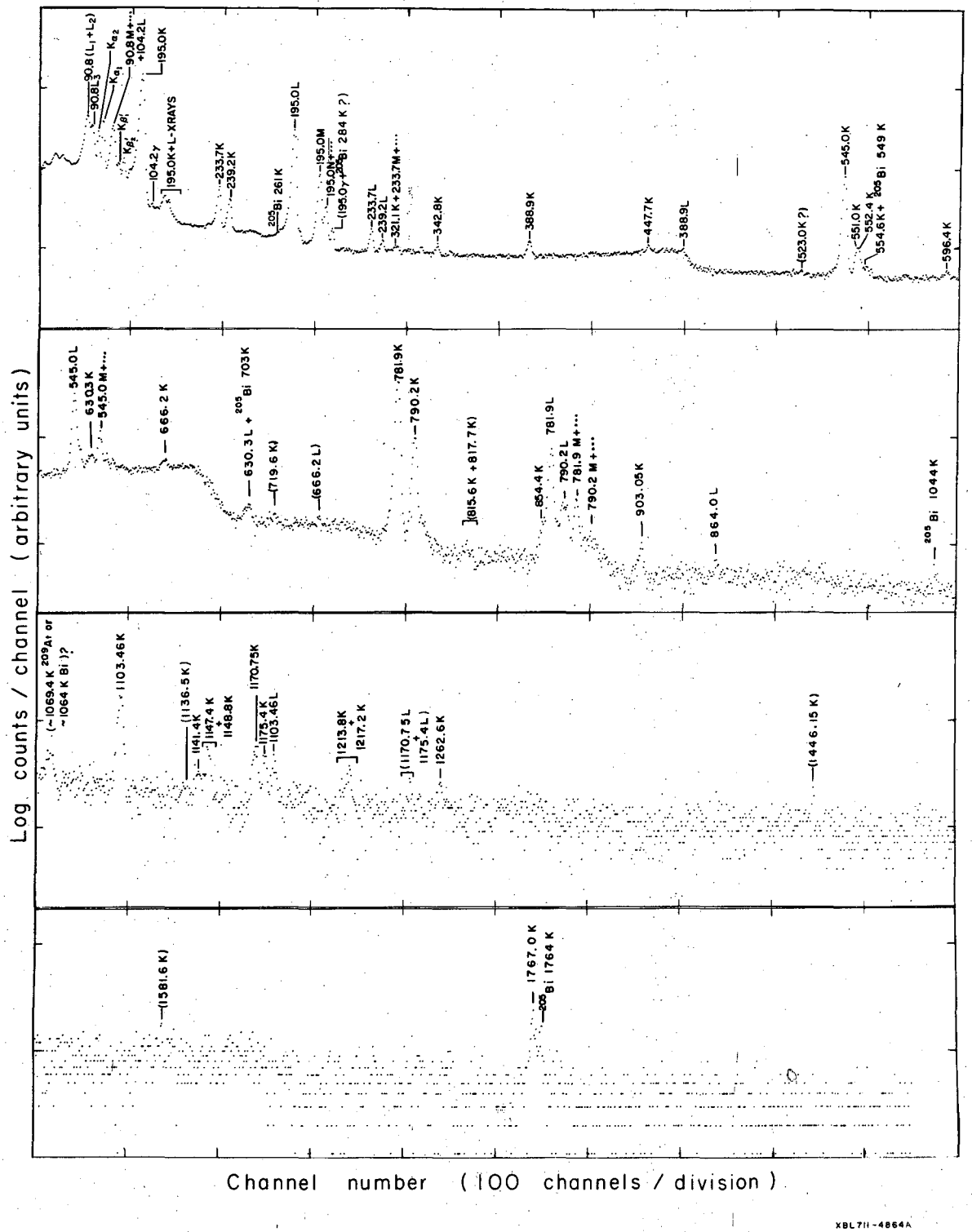
Log counts / channel (arbitrary units)
Channel number (100 channels / division)
90.8 (L1+L2)
90.8 L3
Kα2
Kα1
90.8 M+...
+104.2 L
195.0 K
Kβ1
Kβ2
104.2 γ
195.0 K+L-XRAYS
233.7 K
239.2 K
205Bi 261 K
195.0 L
195.0 M
195.0 N+...
195.0γ, 205Bi 284 K ?)
233.7 L
239.2 L
321.1 K + 233.7 M+...
342.8 K
388.9 K
447.7 K
388.9 L
(523.0 K ?)
545.0 K
551.0 K
552.4 K
554.6 K+ 205Bi 549 K
596.4 K
545.0 L
630.3 K
545.0 M+...
666.2 K
630.3 L + 205Bi 703 K
(719.6 K)
(666.2 L)
781.9 K
790.2 K
(815.6 K +817.7 K)
854.4 K
781.9 L
790.2 L
781.9 M+...
790.2 M+...
903.05 K
864.0 L
205Bi 1044 K
(~1069.4 K 209At or ~1064 K Bi)?
1103.46 K
(1136.5 K)
1141.4 K
1147.4 K
1148.8 K
1170.75 K
1175.4 K
1103.46 L
1213.8 K
1217.2 K
(1170.75 L
1175.4 L)
1262.6 K
(1446.15 K)
(1581.6 K)
1767.0 K
205Bi 1764 K
XBL711-4864A

Fig. 5

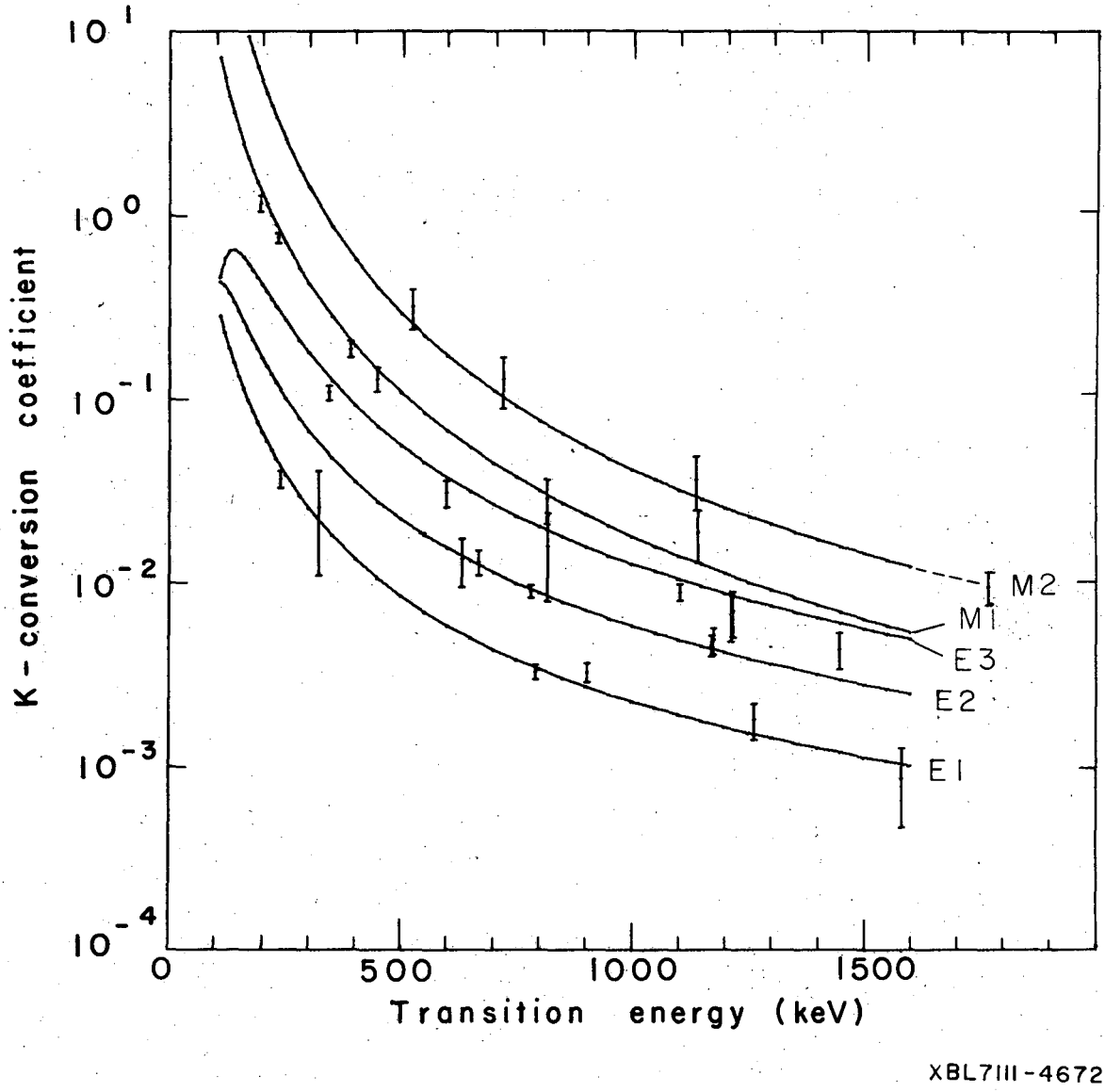
K - conversion coefficient
10^{1}
10^{0}
10^{-1}
10^{-2}
10^{-3}
10^{-4}
0
500
1000
1500
Transition energy (keV)
M2
M1
E3
E2
E1
XBL7111-4672

Fig. 6

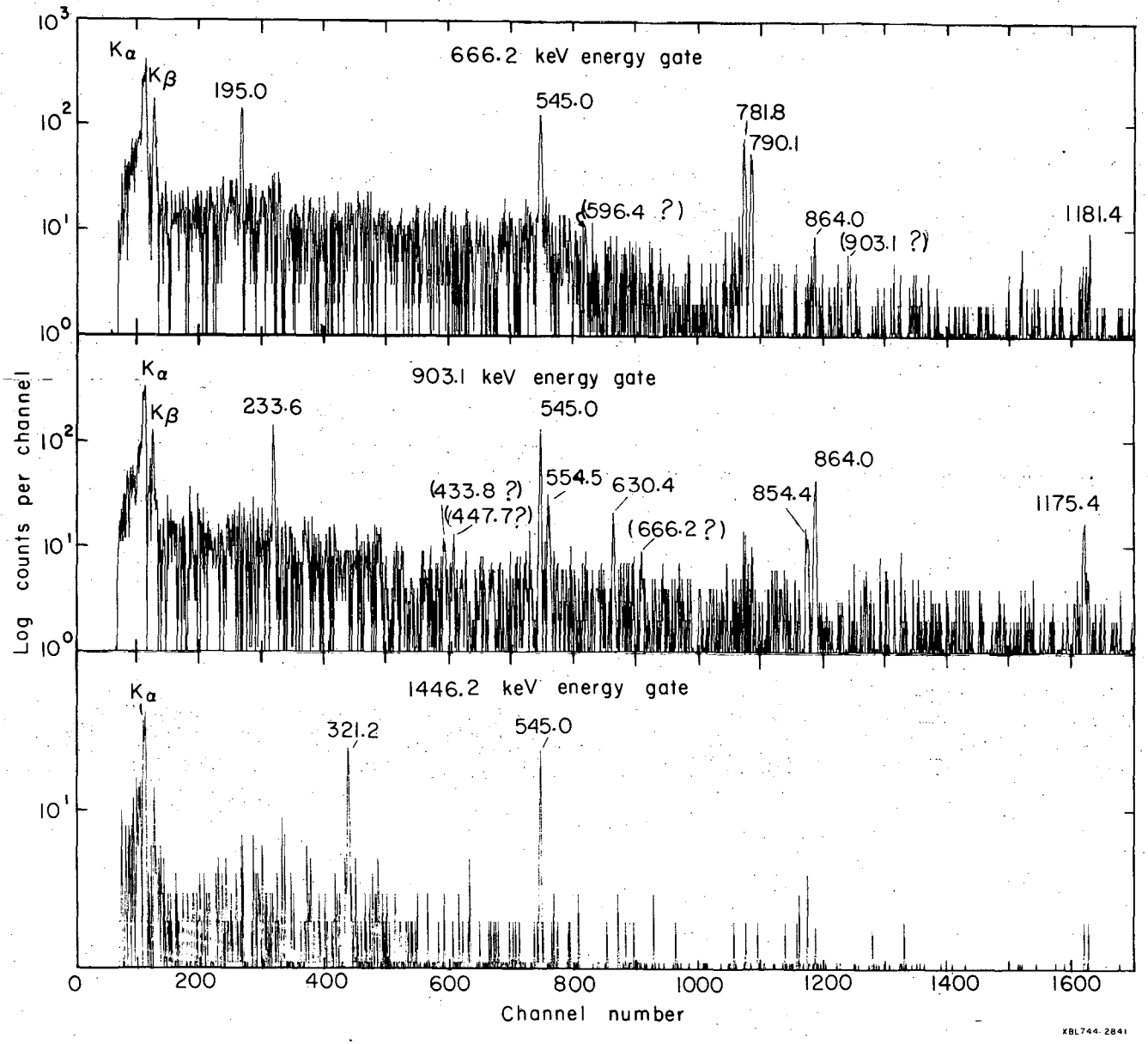
666.2 keV energy gate
Kα
Kβ
195.0
545.0
781.8
790.1
(596.4 ?)
864.0
(903.1 ?)
1181.4
903.1 keV energy gate
233.6
545.0
554.5
630.4
(433.8 ?)
(447.7?)
(666.2 ?)
854.4
864.0
1175.4
1446.2 keV energy gate
321.2
545.0
Log counts per channel
Channel number
XBL744-2841

Fig. 7

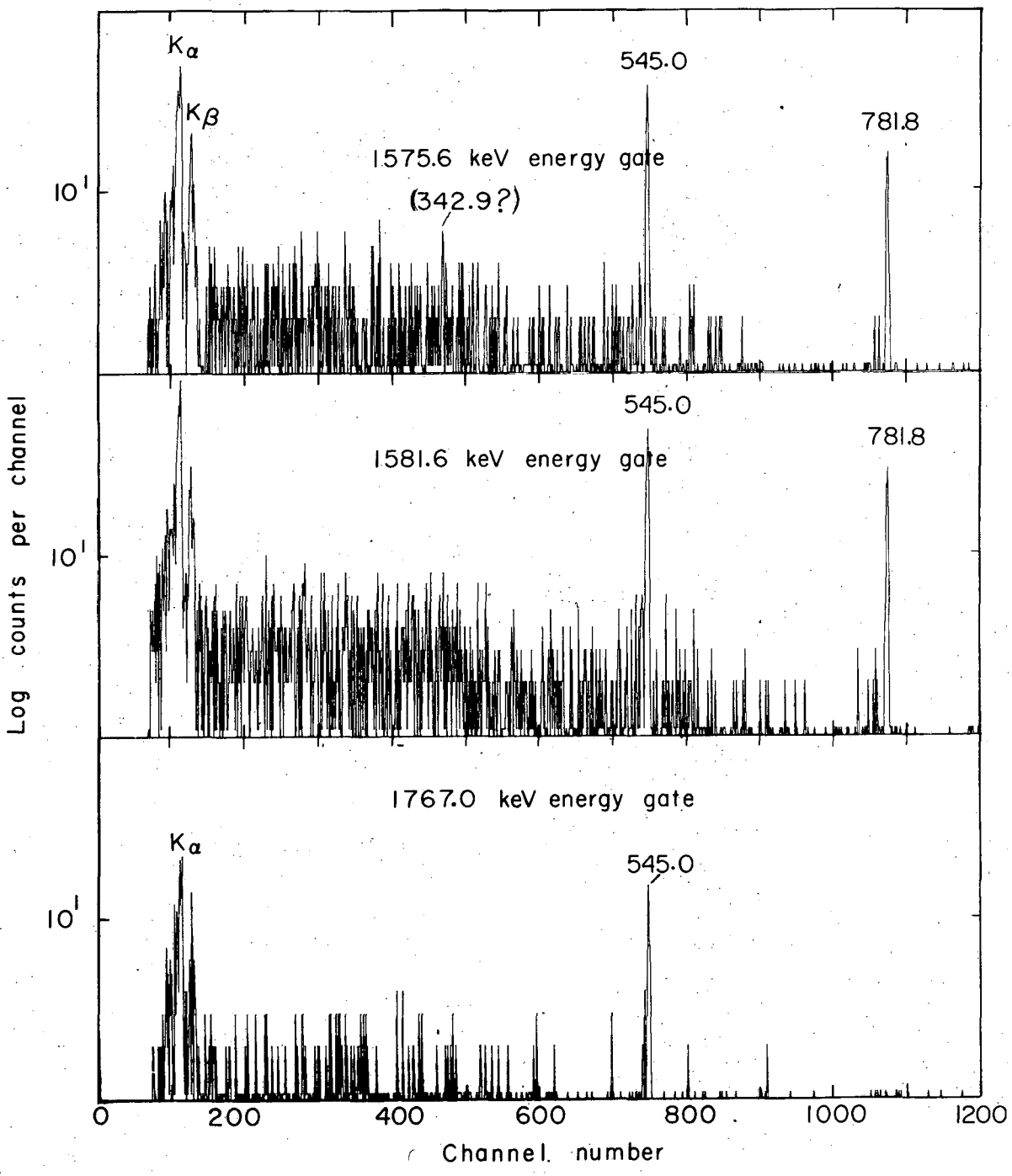
Kα
Kβ
545.0
781.8
1575.6 keV energy gate
(342.9?)
545.0
781.8
1581.6 keV energy gate
1767.0 keV energy gate
Kα
545.0
Log counts per channel
10¹
10¹
10¹
0
200
400
600
800
1000
1200
Channel number
XBL744-2842

Fig. 8

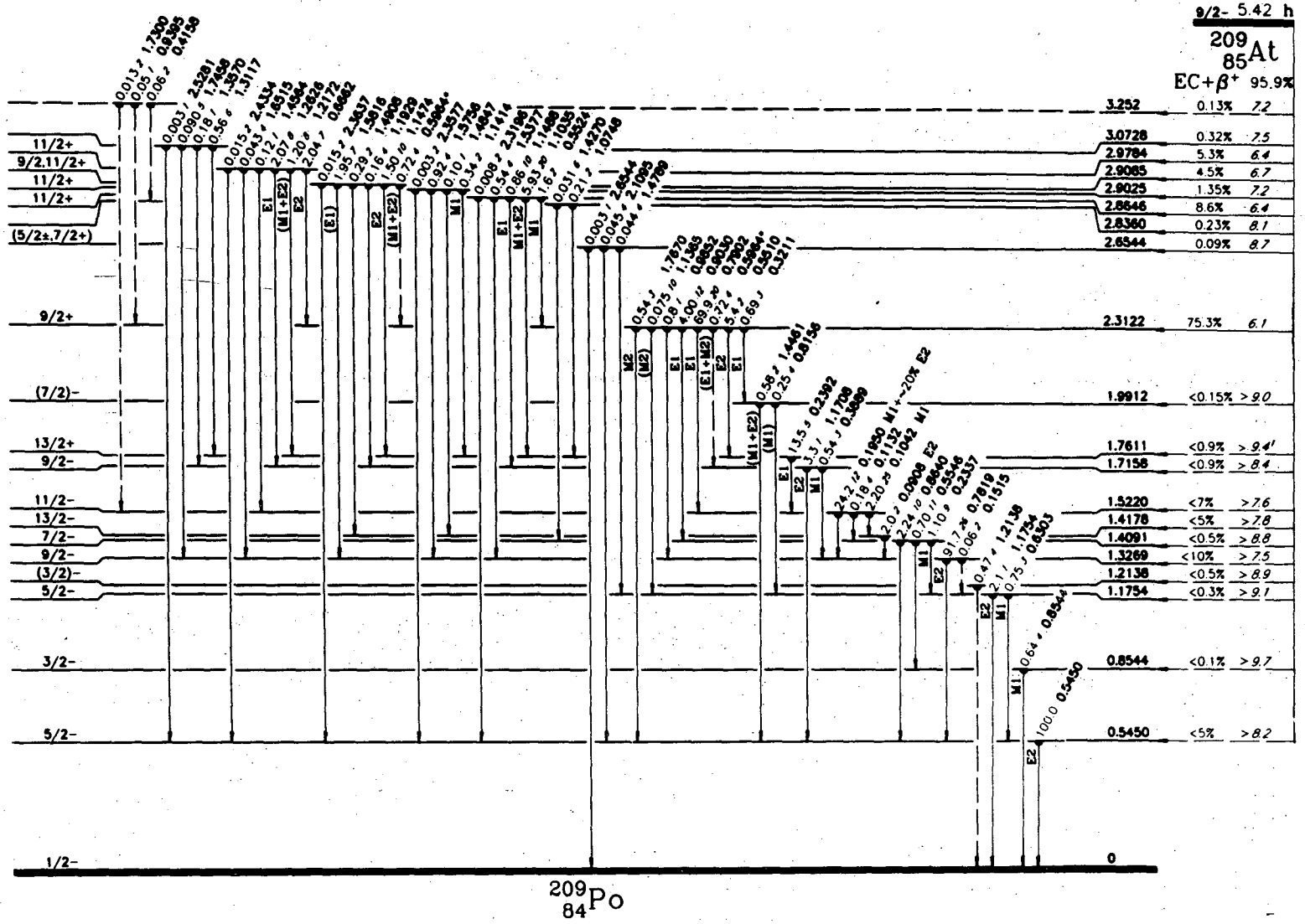

XBL 744-662

Fig. 9

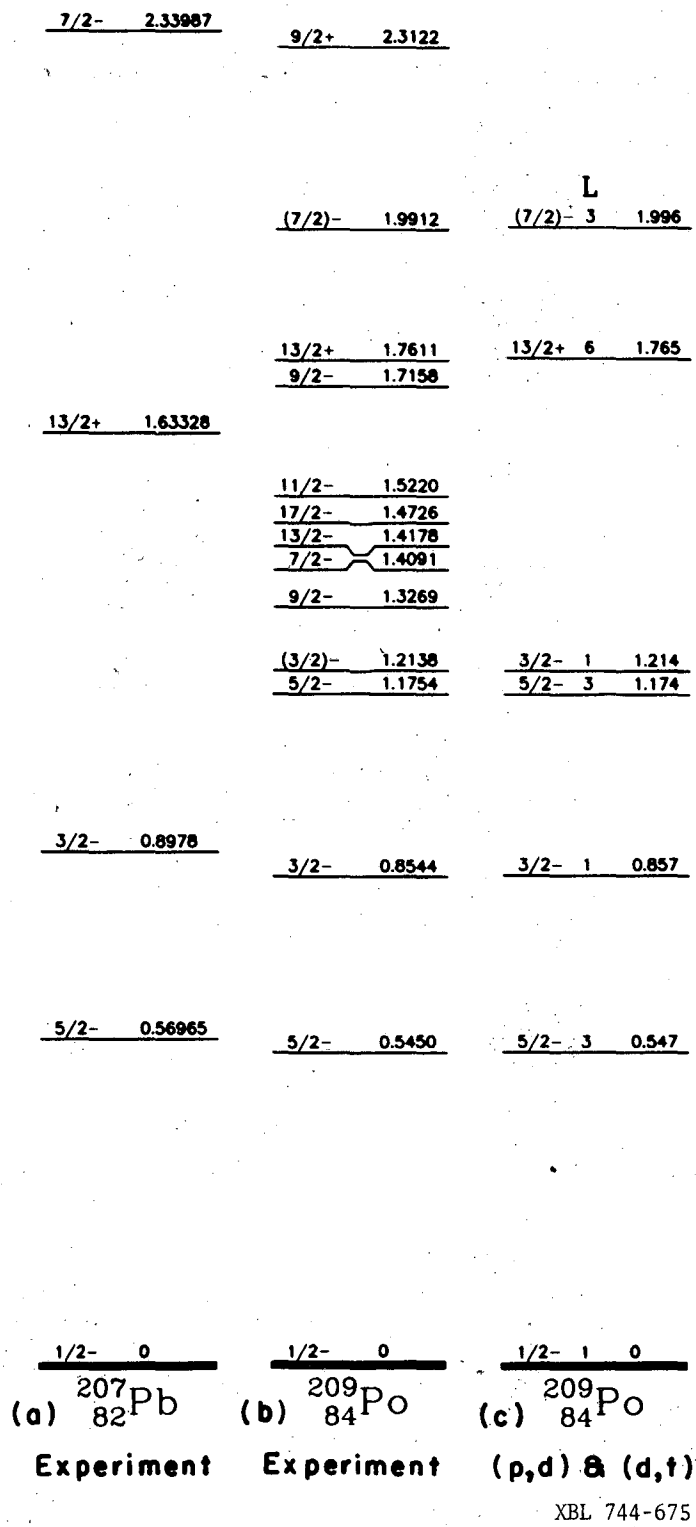
7/2- 2.33987
9/2+ 2.3122
L
(7/2)- 1.9912
(7/2)- 3 1.996
13/2+ 1.7611
9/2- 1.7158
13/2+ 6 1.765
13/2+ 1.63328
11/2- 1.5220
17/2- 1.4726
13/2- 1.4178
7/2- 1.4091
9/2- 1.3269
(3/2)- 1.2138
5/2- 1.1754
3/2- 1 1.214
5/2- 3 1.174
3/2- 0.8978
3/2- 0.8544
3/2- 1 0.857
5/2- 0.56965
5/2- 0.5450
5/2- 3 0.547
1/2- 0
1/2- 0
1/2- 1 0
(a) 207 82Pb
(b) 209 84Po
(c) 209 84Po
Experiment
Experiment
(p,d) & (d,t)
XBL 744-675

Fig. 10

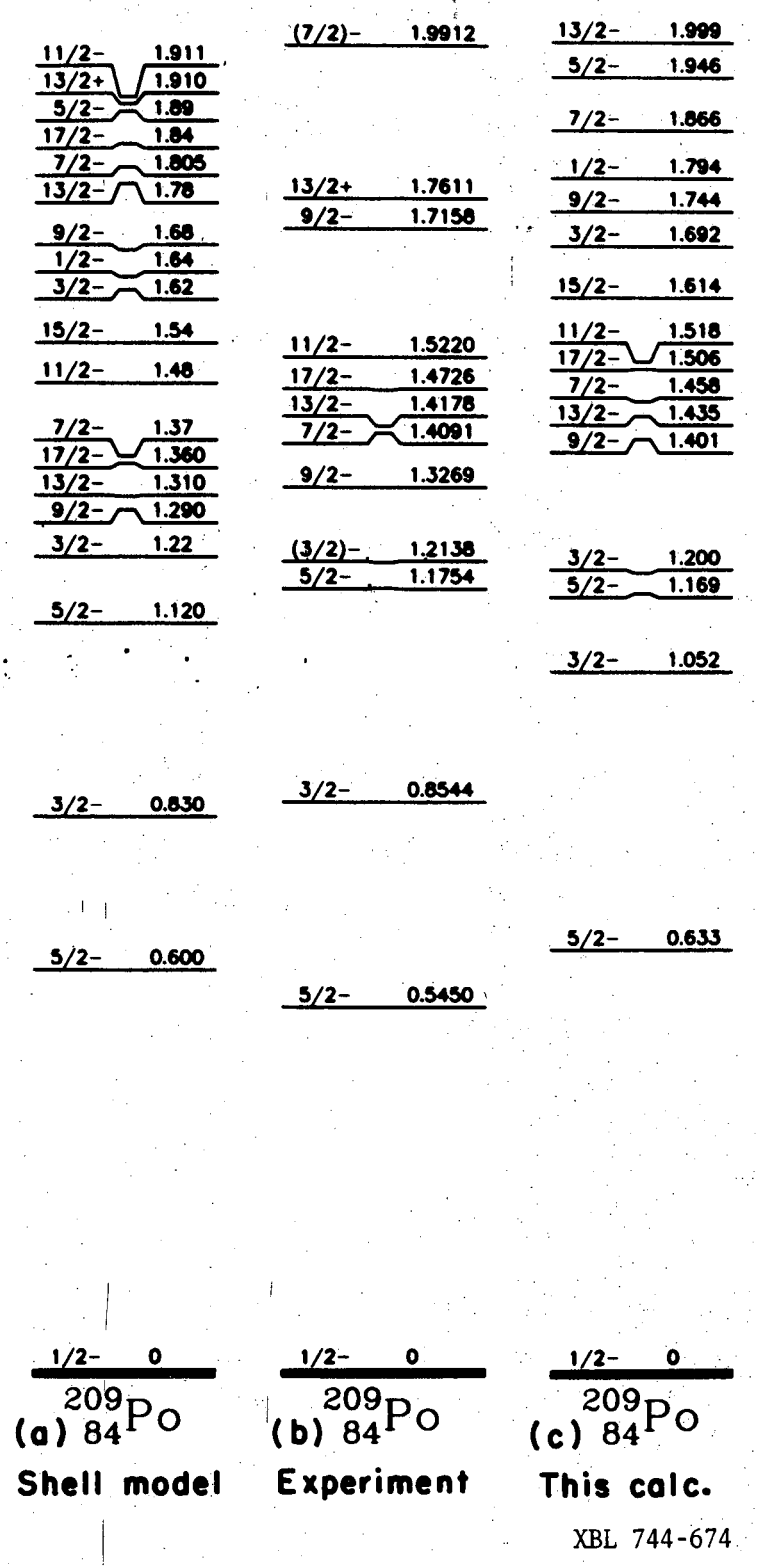
11/2- 1.911
13/2+ 1.910
5/2- 1.89
17/2- 1.84
7/2- 1.805
13/2- 1.78
9/2- 1.68
1/2- 1.64
3/2- 1.62
15/2- 1.54
11/2- 1.48
7/2- 1.37
17/2- 1.360
13/2- 1.310
9/2- 1.290
3/2- 1.22
5/2- 1.120
3/2- 0.630
5/2- 0.600
1/2- 0
(7/2)- 1.9912
13/2+ 1.7611
9/2- 1.7158
11/2- 1.5220
17/2- 1.4726
13/2- 1.4178
7/2- 1.4091
9/2- 1.3269
(3/2)- 1.2138
5/2- 1.1754
3/2- 0.8544
5/2- 0.5450
1/2- 0
13/2- 1.999
5/2- 1.946
7/2- 1.866
1/2- 1.794
9/2- 1.744
3/2- 1.692
15/2- 1.614
11/2- 1.518
17/2- 1.506
7/2- 1.458
13/2- 1.435
9/2- 1.401
3/2- 1.200
5/2- 1.169
3/2- 1.052
5/2- 0.633
1/2- 0
(a) 209 84Po
Shell model
(b) 209 84Po
Experiment
(c) 209 84Po
This calc.
XBL 744-674

Fig. 11

TECHNICAL INFORMATION DIVISION
LAWRENCE BERKELEY LABORATORY
UNIVERSITY OF CALIFORNIA
BERKELEY, CALIFORNIA 94720